

# Power Quality Improvement of AC Distribution System using PV- UPQC with Modified p-q Theory Based Control

T. Satheesh Kumar<sup>1</sup>, Kola Leleedhar Rao<sup>2</sup>,

1PG Scholar, EEE Department, Sree Vidyanikethan Engineering College (Autonomous), Andhra Pradesh, India

2Assistant Professor, EEE Department, Sree Vidyanikethan Engineering College (Autonomous), Andhra Pradesh, India

**Abstract:** This paper proposes a modified p-q theory based control of solar photovoltaic (PV) array integrated unified power quality conditioner (PV-UPQC-S). The system incorporates clean energy generation along with power quality improvement thus increasing functionality of the system. The fundamental frequency positive sequence (FFPS) components of voltages at the point of common coupling (PCC) are extracted using generalized cascaded delay signal cancellation (GCDSC) techniques which are then used in p-q theory based control to estimate reference signals for the PV-UPQC-S. This modification in p-q theory enables its application for PV-UPQC-S control in conditions of distorted PCC voltages. The series voltage source converter (VSC) of PVUPQC- S operates such that it shares a part of the reactive power of the load even under nominal grid conditions. This increases the utilization of the series VSC while reducing the rating of shunt VSC. The PV array is integrated at the DC-bus of the UPQC, provides a part of active load power thus reducing demand on the supply system. The dynamic performance of modified p-q theory based PV-UPQC-S is verified by simulating the system in Matlab/Simulink with combination of linear and nonlinear loads. The steady state and dynamic performances of the system validated through extensive testing on a scaled down laboratory prototype.

**Index Terms**—power quality, UPQC-S, solar MPPT, GCDSC, p-q theory, series compensation, shunt compensation.

## I INTRODUCTION

There is an increasing need for renewable energy systems with ancillary features particularly in low voltage distribution systems. This is due to the fact that there is an increased penetration of nonlinear power electronics based loads and renewable energy based systems [1]–[3]. These power electronic loads though energy efficient, inject harmonic currents into grid which cause distortion at point of common coupling (PCC) particularly in weak grid systems. Moreover, these power electronic loads are sensitive to disturbances in voltages. In weak distribution systems, due to the intermittent nature of the clean energy sources such as wind and solar energy, their increased penetration leads to PCC voltage fluctuations depending upon power generation and demand. These voltage fluctuations can affect sensitive power electronic loads such as adjustable speed drives, lighting systems etc which can lead to frequent tripping, mal operation and thus leading to increased maintenance costs.

Renewable energy integration with power quality enhancing systems such as dynamic voltage restorer (DVR), unified power quality conditioner (UPQC) and distribution static compensator (DSTATCOM) provides an ideal solution by combining benefits of clean energy with power quality enhancement. Most of the research on renewable energy system with power quality improvement has been carried out in case of shunt voltage source converter (VSC) based systems. A solar PV integrated shunt VSC with DSTATCOM functionalities such as grid current power quality improvement has been proposed in [4], [5]. A novel topology of PV and DVR systems with reduced number of switches has been proposed in [6]. Though DSTATCOM can also perform voltage regulation, it comes at the cost drawing reactive power from the PCC. Moreover, DSTATCOM cannot protect load from harmonics in PCC voltage. UPQC with its series and shunt VSCs, provides both load voltage regulation as well as improvement in grid current quality. UPQC provides a complete solution for mitigating both the load side and PCC side power quality issues [7]. A detailed review of various UPQC configurations and control has been given in [8]. UPQCs are classified into three categories based on the angle between the voltage injected by the series VSC and the grid current, namely

- UPQC-P: The series voltage is injected in-phase with grid current and hence it results in active power consumptions by the series compensator.
- UPQC-Q: The series voltage is injected in quadrature with the grid current and hence it results in consumption of only reactive power by the series compensator.
- UPQC-S: The series voltage is injected at an appropriate angle based on operational requirements and hence it results in consumption of both reactive and active powers.

In conventional UPQC which is UPQC-P, the series VSC remains idle during nominal conditions [9]. In this work, the series VSC shares a part of reactive power of the load during nominal and sag conditions. This increases the utilization of the series VSC while reducing the loading on the shunt VSC. The concept of sharing reactive power of load has been investigated extensively in [10]. However, the authors have considered UPQC under ideal PCC voltage conditions. In this work, performance analysis of PV-UPQC-S is carried out under distorted PCC voltage conditions along with nonlinear loads. Moreover, PV array is integrated at the DC-link of UPQC to provide clean energy for the load and also to reduce the demand on the supply system. An integration of distributed generation particularly PV array at the DC-bus of UPQC has been theoretically investigated in [11], [12].

The integration of PV system brings additional constraints in sharing of reactive power by the series VSC to prevent its excessive voltage rating. This is further analyzed in describing series VSC control. The major tasks in control of PV-UPQC-S are reference signal estimation for the shunt and series VSCs. The reference signals for the shunt VSC are PCC currents which should be sinusoidal and at unity power factor while the series VSC voltages should be such that it compensates for sags/swells and harmonics in PCC voltages. The most commonly used algorithms for reference signal estimation are time domain based techniques. These include p-q theory, d-q theory and instantaneous symmetrical components theory [13], [14]. Some other advanced control techniques for reference signal generation include

using adaptive filters such as adaptive notch filter (ANF), adaptive linear element (ADALINE) etc. [15]–[17]. However, these methods require calculations for each of the phase currents and voltages and are more complex compared to methods based on p-q or d-q theories which are inherently three-phase based techniques.

In control of PV-UPQC-S, p-q theory based technique is ideal as this technique inherently calculates load active and reactive powers which are necessary in particularly in reactive power sharing of series VSC. Though the classical p-q theory involves only simple calculations, it does not produce accurate results under conditions of voltage distortions or unbalance [18]. This drawback can be overcome by using fundamental frequency positive sequence (FFPS) voltages for estimating the reference currents using p-q theory. Modified p-q theory using phase locked loop (PLL) has been proposed in [19]. Various other methods to extract fundamental frequency positive sequence voltages are using notch filters [20], second order generalized integrators (SOGI) [21], generalized cascaded delay signal cancellation (GCDSC) based methods [22] etc. Techniques based on adaptive notch filters use a number of filter blocks for each harmonic component and have a slower response time which results in a settling time of a few cycles [23]. The performance of SOGI based techniques deteriorates greatly with minor deviations from their tuned frequencies [24]. The techniques based on GCDSC have improved harmonic attenuation characteristics. Moreover, these techniques are also insensitive to minor variation in frequency and have a reported settling time of 0.3 cycles [24]. In this work, GCDSC technique is integrated with p-q theory to improve the operating performance of PV-UPQCS under distorted PCC voltage conditions. This improves the performance of p-q theory particularly under distorted grid conditions. The shunt VSC of the system compensates for load current harmonics, a part of load reactive power and also injects active power from PV array.

The DC-link of PVUPQC- S is maintained by the shunt VSC. The reference for the DC link voltage is obtained using maximum power point tracking algorithm [25]. The series VSC protects sensitive load from fluctuations and distortions in PCC voltage. The main contributions of this work are as follows

- A modified p-q theory algorithm based on GCDSC enables operation of PV-UPQC-S under polluted PCC voltage conditions.
- The integration of PV array at the DC-link of PV-UPQC reduces the load demand on supply system
- The reactive power sharing by the series VSC increases utilization of series VSC under nominal conditions while reducing the burden on shunt VSC.
- Analysis on the impact of reactive power sharing capability of series compensator under PV integration.
- Experimental evaluation of steady state and dynamic performances of PV-UPQC-S system under various disturbance conditions.

The proposed modified p-q theory based PV-UPQC-S is simulated using Matlab/Simulink and its dynamic performance is tested under conditions of irradiation variation, voltage sags/swells, distortions, load unbalance etc. The response of the PV-UPQC-S under steady state and dynamic conditions is then experimentally validated using a scaled down laboratory prototype.

Several control techniques had developed for improving the PQ using UPQC and other custom power devices. But still less attention is paid on improving the utilization factor of series APF which is increasing the rating and cost of UPQC and ability to mitigate the long term power quality problems such as voltage sag/swell, interruption, harmonics and reactive power. These became primarily motivation for the current project.

## II BASIC STRUCTURE OF PV-UPQC-S

The topology of a PV-UPQC-S is presented in Fig. 1. The major components of the system are a series VSC and shunt VSC connected back to back through a prevalent DC-bus. The VSCs are connected to PCC utilizing interfacing inductors. Ripple filters are habituated to filter out switching harmonics of the VSCs. The series VSC injects voltage through a series injection transformer. The PV array is connected directly at the DC-bus of UPQC through a inversion blocking diode.

The phasor diagram of the PV-UPQC-S with a linear reactive load is presented in Fig. 1.5. The subscript '1' represents condition when reactive power is shared by shunt VSC only whereas the subscript '2' refers to condition when the series VSC shares a component of reactive load puissance. The PCC voltage ( $V_{S1}$ ) and load voltage ( $V_{L1}$ ) are in phase when series VSC is not injecting any voltage. The load current afore series emolument is ( $I_{L1}$ ) and the load angle is ( $\phi$ ).

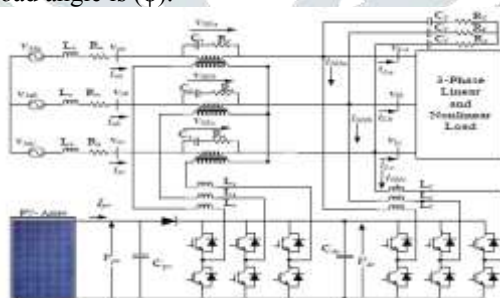


Fig: 1 Structure of PV-UPQC-S

The shunt VSC withal injects authentic power obtained from PV array which is represented by ( $I_{PV}$ ). The remaining part of the load authentic power is obtained from the grid ( $I_{S1}$ ). The shunt VSC current ( $I_{SH1}$ ) afore series VSC injection is phasor sum of PV array current and load reactive current. When a component of reactive power of the load is to be shared by series VSC, then series VSC injects voltage ( $V_{SE}$ ) such that load voltage is shifted to ( $V_{L2}$ ). This results in shifting of load current to ( $I_{L2}$ ). However, as the active current drawn from the grid is to remain same ( $I_{S1} = I_{S2} = I_S$ ), the shunt VSC current reduces to ( $I_{SH2}$ ). It can be observed that due to power angle ( $\delta$ ), the component of reactive encumbrance of shunt VSC is shared by the series VSC thus incrementing the utilization of series VSC.

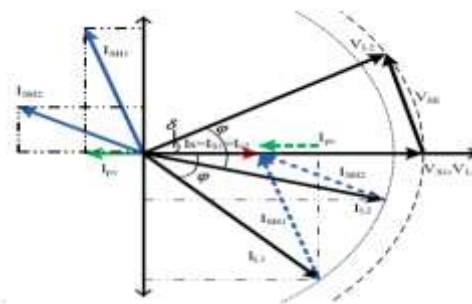


Fig: 2 Phasor Diagram of PVUPQC-S

For a given reactive power sharing by series VSC, the magnitude of series VSC voltage  $V_{SE}$  is lesser under sag condition as compared to swell condition. This is because the grid current  $I_S$  is higher under sag condition as compared to swell condition for a constant load. Predicated on these observations, in order to obviate extortionate VA rating of series VSC, the control implemented is such that, it compensates for reactive power under sag and nominal conditions. The PV array is designed such that it supplies around 30% of load active potency. This is because as more load active power is supplied by the PV array, there is less current drawn from the grid which reduces the reactive power sharing capability of series VSC for a fine-tuned voltage rating of series VSC. The consummate design parameters of PV-UPQC-S.

### III CONTROL DESIGN OF PV-UPQC-S

There are four control blocks involved in the control of PVUPQC- S. These are GCDSC block, load power calculation block, shunt VSC and series VSC control block. These are elaborated as follows:

#### (a) Generalized Cascaded Delay Signal Cancellation Block

A delay signal cancellation (DSC) operator [22] for extraction of FFPS component of voltage is given as,

$$v_{h\alpha-\beta}(t) = \frac{1}{2} \left[ v_{\alpha-\beta}(t) + e^{j\frac{2\pi}{N}} v_{\alpha-\beta}(t - \frac{T}{N}) \right] \quad (1)$$

Where  $V_{\alpha-\beta}(t) = V_{\alpha} + jv_{\beta}(t)$  is the voltage vector in  $\alpha, \beta$  frame,  $v_{h\alpha-\beta}(t) = v_{h\alpha}(t) + jv_{h\beta}(t)$  is the FFPS component of voltage along with harmonics of order  $h = N \times k + 1$  ( $k = \pm 1, \pm 2, \pm 3, \dots$ ) in  $\alpha-\beta$  domain,  $T$  is the fundamental period of voltage,  $N$  is the delay factor. The transfer function of DSC operator is given as,

$$G_N(j\omega) = \left| \cos\left(\frac{\omega T}{2N} - \frac{\pi}{N}\right) \right| \angle -\left(\frac{\omega T}{2N} - \frac{\pi}{N}\right) \quad (2)$$

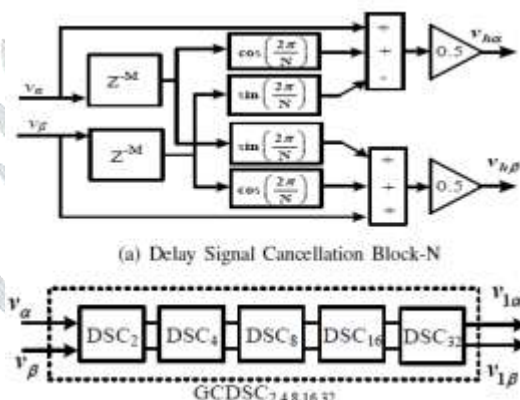


Fig: 3. Fundamental Frequency Positive Sequence Extraction using Generalized Cascaded Delay Signal operation

A delay factor  $N$  blocks harmonics of the order  $h_b = N \times k - 1$  ( $k = \pm 1, \pm 2, \pm 3, \dots$ ). The mathematical implementation of DSC operator is presented in Fig. 3.3(a). As it can be observed from the figure, in discrete form, the delay is implemented by  $z^{-M}$  where  $M$  is delay samples corresponding to a delay factor of  $N$ . When the harmonic content of PCC voltage is unknown, it is often recommended to cascade five delay signal operator blocks with delay factors  $N = 2, 4, 8, 16, 32$ . This system of cascaded blocks is kenne as GCDSC block as represented in Fig. 1.6(b).

The system can be made frequency adaptive, by utilizing GCDSC block as a prefiltering scheme as in case of GCDSCPLL [22]. When the GDSC is designed for a frequency of 50Hz, a signal of 49Hz is attenuated by 0.065% and phase error of  $3.43^\circ$  as it can be obtained from (2). Since the mundane grid fundamental frequency variation emanates from 49.3 to 50.2 Hz [26], this variation causes only negligible magnitude and phase error. Hence, frequency adaptation can be evaded to obviate nonessential involution in the system. The magnitude replication of GCDSC is shown in Fig. 1.7. The frequency axis in the plot is normalized with veneration to 50Hz frequency. It can be visually perceived that GCDSC sanctions only FFPS components and substantially attenuates lower order harmonics. However, certain harmonics which are expressed as  $h = 32 \times k + 1$ , ( $k = \pm 1, \pm 2, \dots$ ) are passed without attenuation (i.e 33rd positive sequence harmonic, 31st negative sequence harmonic etc.). Mundanely, the magnitude of such components is negligible. However, they can still cause error in calculation of phase and magnitude information. Hence a band-pass filter (BPF) is withal used to abstract these high frequency signals from FFPS signal obtained utilizing GCDSC.



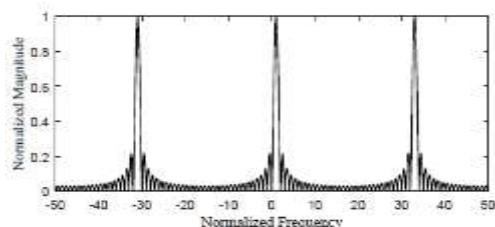


Fig: 4 Magnitude Response of GCDSC

### (b) Load Power Calculation Block

This block calculates the instantaneous active and reactive load powers using p-q theory. The block diagram of load power calculation is shown in Fig. 1.8. The load voltages ( $v_{La}$ ,  $v_{Lb}$ ,  $v_{Lc}$ ) and load currents ( $i_{La}$ ,  $i_{Lb}$ ,  $i_{Lc}$ ) are converted into  $\alpha - \beta$  domain load voltages ( $v_{L\alpha}$ ,  $v_{L\beta}$ ) and load currents ( $i_{L\alpha}$ ,  $i_{L\beta}$ ) using power invariant Clarke transform. The instantaneous active and reactive powers,  $p_L$  and  $q_L$  are passed through low-pass filter (LPF) to obtain fundamental active and reactive powers  $PL$  and  $QL$ .

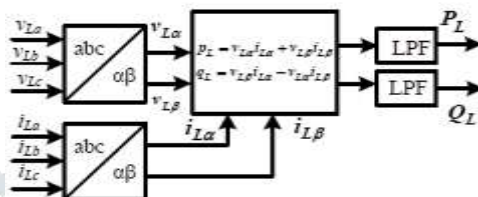


Fig: 5. Block diagram of Power Block

### (c) Shunt VSC Control Structure

The shunt VSC control block diagram is presented in Fig. 1.9. The shunt VSC mitigates the current power quality problems at load side such as unbalanced loading, distorted current and poor power factor. Along with this, it also injects real power obtained from PV array into the grid and maintains the DC-bus voltage at MPP voltage of the PV array. The reference value for the DC-bus voltage is obtained from MPPT algorithm. In this work, perturb and observe (P&O) algorithm is used to extract maximum power from the PV array. The sensed DC-bus voltage ( $V_{dc}$ ) is passed through LPF and is compared with reference DC-bus voltage ( $V^*_{dc}$ ). The error between  $V_{dc}$  and  $V^*_{dc}$  is passed through proportional integral (PI)-controller which gives the loss component ( $P_{loss}$ ). The power ( $P_{ref}$ ) to be drawn from the grid is given as,

$$P_{ref} = PL + P_{loss} - P_{pv} \quad (3)$$

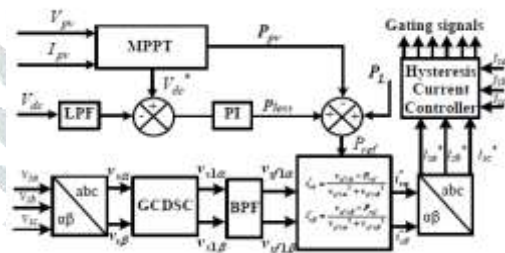


Fig:6 Shunt VSC Control Structure

The FFPS components of PCC voltages  $vs1\alpha$ ,  $vs1\beta$  obtained using GCDSC block are filtered using band pass filters to give  $vsf1\alpha$ ,  $vsf1\beta$ . The reference grid currents in  $\alpha - \beta$  frame are calculated using  $P_{ref}$  and  $vsf1\alpha$ ,  $vsf1\beta$  as,

$$i^*_{\alpha} = \frac{vsf1\alpha \times P_{ref}}{vsf1\alpha^2 + vsf1\beta^2} \quad (4)$$

$$i^*_{\beta} = \frac{vsf1\beta \times P_{ref}}{vsf1\alpha^2 + vsf1\beta^2} \quad (5)$$

These calculated reference signals are converted to abc domain and compared with sensed grid currents ( $isa$ ,  $isb$ ,  $isc$ ) in a hysteresis current controller to generate gating signals for the shunt VSC.

### (d) Control of Series VSC

The series VSC control block diagram is presented in Fig. 2.0. The series VSC, apart from protecting the sensitive loads from PCC voltage sags/swells, compensates for a part of the load reactive power even under nominal PCC voltage conditions. The relationship between power angle  $\delta$  and reactive power shared by series VSC ( $Q_{SE}$ ) under nominal condition [10] is given as follows,

$$\delta = \arcsin \left[ \frac{Q_L - Q_{SH}}{P_L - P_{PV}} \right] \quad (6)$$

Where  $Q_{SH}$  is a preset parameter which is amount of reactive power to be shared by the shunt VSC,  $Q_L$  is average load reactive power,  $P_L$  is average load active power and  $P_{PV}$  is PV array power. Under conditions of PCC voltage sag and swell, the expression is modified as follows,

$$\delta = \arcsin \left[ \frac{Q_L - Q_{SH}}{K(P_L - P_{PV})} \right] \quad (7)$$

Where  $K$  is ratio of load reference voltage peak  $V^*_{L}$  upon PCC voltage peak  $V_S$ . The magnitude of  $(Q_L - Q_{SH})$  should be always lesser than  $(P_L - P_{PV})$  for validity of (7). For same reactive power sharing by series VSC, the power angle  $\delta$  is less when  $P_{PV}$  is lesser and vice-versa. Using  $vsf1\alpha$ ,  $vsf1\beta$  components, the peak of PCC fundamental voltage ( $V_S$ ) and its phase ( $\theta$ ) are obtained. The ratio of  $V_S$  upon  $V$

\*  $L$  gives factor  $K$ . Factor  $K_d$  is obtained after mathematical operation of 'floor' on  $K$ . The value of  $K_d$  is 0 under swell condition and 1 under sag condition. Basically this is done so that reactive power sharing is done only in sag and nominal conditions.

Though the series VSC can compensate load reactive power during voltage swell conditions, the PCC current decreases under swell condition and hence a higher magnitude of voltage needs to be injected for same reactive power compensation. This results in higher voltage rating of series compensators. As the occurrence of voltage swell is very much lesser as compared to that of voltage sags, it is decided in the control algorithm to avoid reactive power compensation during swell conditions and it only performs voltage swell compensation.

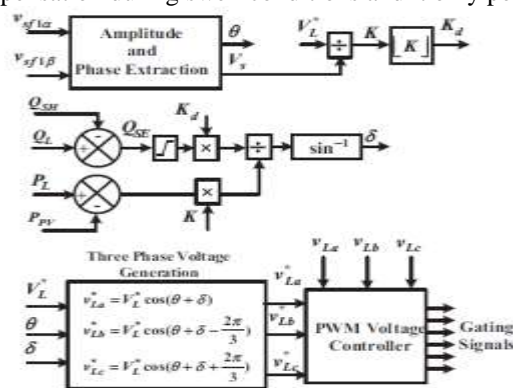


Fig: 6 Series VSC Control Structure

There is a saturation block to keep lower limit of  $Q_{SE}$  to zero. Thus if the load reactive power is less than that of  $Q_{SH}$ , then the entire reactive power is shared by shunt VSC. The power angle  $\delta$  is calculated based on (7).

The reference load voltage are then used in a pulse width modulated (PWM) voltage controller to generate gating signals for the series VSC.

#### IV MATLAB SIMULINK RESULTS & DISCUSSIONS

The dynamic demean or PV-UPQC-S under dynamic conditions is simulated in Matlab/Simulink software utilizing SimPowerSystems block set. The dynamic performance is evaluated at different conditions such as fluctuation in PCC voltages, irradiation variation and load unbalance conditions. The load used is a accumulation of linear and nonlinear loads.

##### A. PV-UPQC-S Performance Under Load Unbalance Condition

The PV-UPQC-S performance during load unbalance condition is presented in Fig.7 The signals shown are PCC voltages ( $v_s$ ), load voltages ( $v_L$ ), DC-bus voltage ( $V_{dc}$ ), grid currents ( $i_s$ ), load currents ( $i_L$ ), shunt VSC currents ( $i_{SH}$ ), PV array power ( $P_{pv}$ ). At 0.51 s the phase 'b' of load is disconnected thus resulting in an unbalanced nonlinear load. It can be observed that the shunt VSC of PV-UPQC-S maintains the grid currents balanced at unity power factor. The DC-bus voltage settles within 0.04 s to its regulated value of 700 V after a slight overshoot of 20 V.

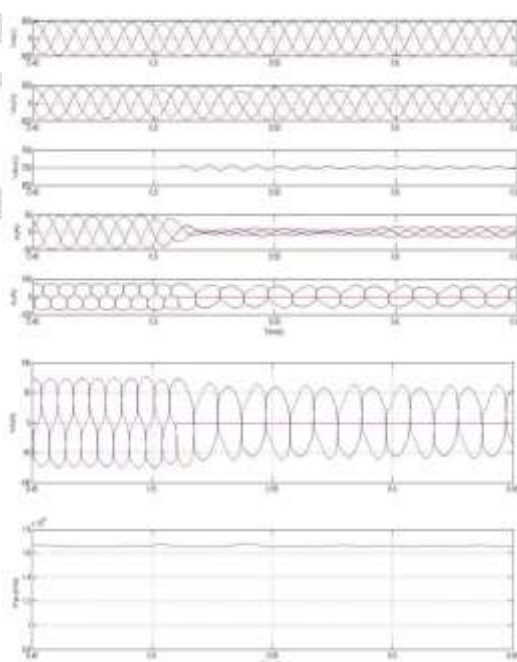
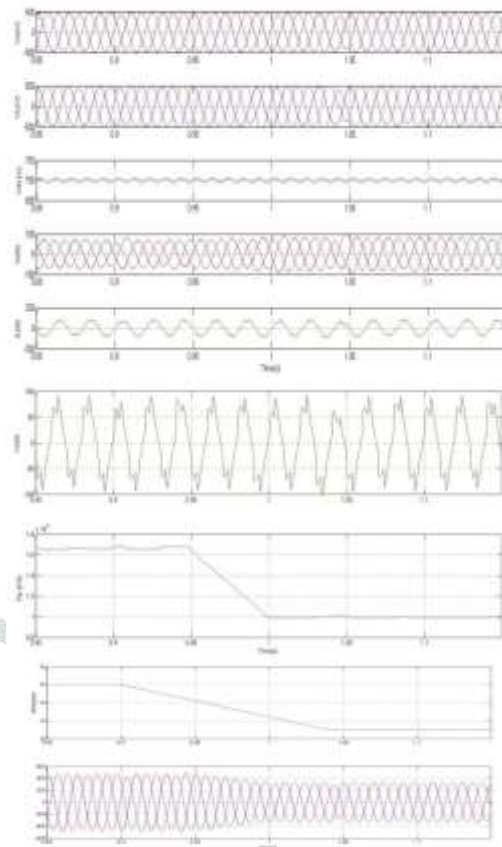


Fig.7. PV-UPQC-S Performance Under Load Unbalance Condition

##### B. PV-UPQC-S Behaviour during Irradiation Change

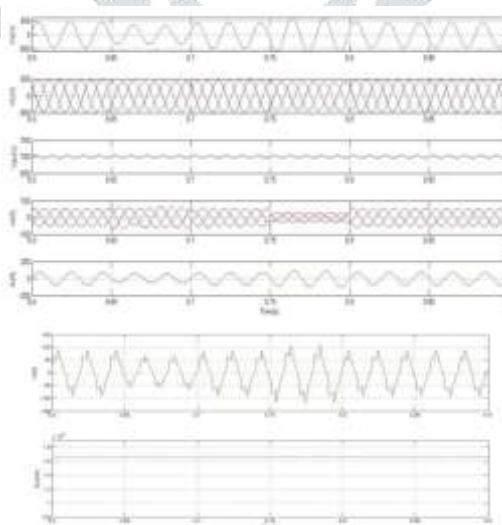
The PV-UPQC-S performance during change in irradiation is presented in Fig.8. The signals shown are PCC voltages ( $v_s$ ), load voltages ( $v_L$ ), DC-bus voltage ( $V_{dc}$ ), grid currents ( $i_s$ ), load currents ( $i_L$ ) of phase 'a', shunt VSC currents ( $i_{SH}$ ) of phase 'a', PV array power ( $P_{pv}$ ), series VSC voltages ( $v_{SE}$ ) and power angle ( $\delta$ ). From 0.95s to 1 s the solar irradiation is varied from 1000 W/m<sup>2</sup> to 500 W/m<sup>2</sup>. As it can be observed from Fig. 9, the power angle and series VSC voltages are higher at higher PV power as compared to lower PV power. This is due the fact that, as the PV array power supplies a part of load real power demand, the grid current drawn is lower. Hence, to compensate the same reactive power, the load angle and series VSC voltage is higher as compared to case when the PV array power is lesser.



**Fig.8. PV-UPQC-S Behaviour during Irradiation Change**

### C. PV-UPQC-S Performance during PCC Voltage Disturbances

The PV-UPQC-S behaviour under PCC voltage disturbance is presented in Fig.2.3. The solar irradiation ( $G$ ) is kept constant at  $1000 \text{ W/m}^2$ . The signals shown are PCC voltage of phase 'a' ( $v_s$ ), load voltages ( $v_L$ ), DC-bus voltage ( $V_{dc}$ ), grid currents ( $i_s$ ), load current ( $i_L$ ), shunt VSC current ( $i_{SH}$ ), PV array power ( $P_{pv}$ ), power angle ( $\delta$ ), series VSC voltages ( $v_{SE}$ ). Only signals of one phase are shown in case of certain signals for clarity in representation. At 0.65 s, there is a voltage sag of 0.3 pu along with harmonic distortion and at 0.75 s there is voltage swell of 0.3 pu along with harmonic distortion. It can be seen that load voltage is sinusoidal and reference value despite the distortions in PCC voltage. Under nominal conditions, as seen from  $\delta$  and  $v_{SE}$  the series VSC still operates to share a part of reactive power of the load. Under swell conditions, the series VSC compensates only swell and no reactive power sharing is done, which is shown by  $\delta$  being zero under voltage swell. After PCC voltage swell, there is a slight delay of 2 cycles for series VSC to calculate necessary power angles. This is due to low pass filters using in  $P_L$  and  $Q_L$  calculation.





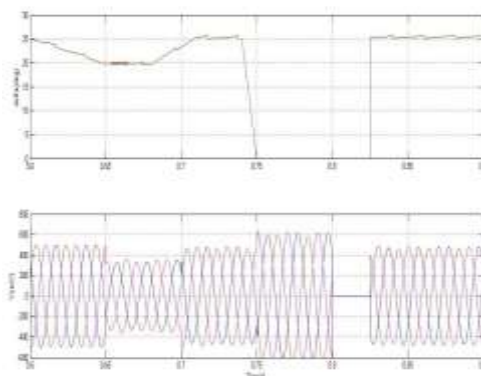


**Fig.9. PV-UPQC-S Performance during PCC Voltage Disturbances**

## V CONCLUSION

The dynamic performance of modified p-q theory predicated PV-UPQC-S has been analyzed in detail. A GCDSC block has been used to extract FFPS component of distorted PCC voltages which is then utilized in control of utilizing p-q theory PV-UPQC-S. The modified p-q theory enables the PV-UPQCS to work under conditions of distorted PCC voltages. The series VSC shares a component of reactive power of the load under nominal conditions thus incrementing utilization of series VSC and additionally reducing the loading on the shunt VSC. The dynamic performance of PV-UPQC-S is shown under scenarios of sudden vicissitude in irradiation and fluctuations in PCC voltage such as voltage sags/swells. The proposed system can work under multiple perturbances such as irradiation variation and PCC voltage perturbances occurring simultaneously. The PVUPQC- S system cumulates concept of clean energy generation along with power quality amelioration thus incrementing its utility.

## REFERENCES

- [1] L. F. de Oliveira Costa and J. M. de Carvalho Filho, "Electrical power quality and the challenges faced by power assemblies applications in petrochemical industry," *IEEE Trans. Ind. Appl.*, vol. 52, no. 5, pp. 4495–4502, Sept 2016.
- [2] A. Banerji, S. K. Biswas, and B. Singh, "Enhancing quality of power to sensitive loads with microgrid," *IEEE Trans. Ind. Appl.*, vol. 52, no. 1, pp. 360–368, Jan 2016.
- [3] H. Hafezi, G. D'Antona, A. Ded, D. D. Giustina, R. Faranda, and G. Massa, "Power quality conditioning in LV distribution networks: Results by field demonstration," *IEEE Transactions on Smart Grid*, vol. 8, no. 1, pp. 418–427, Jan 2017.
- [4] R. K. Agarwal, I. Hussain, and B. Singh, "Three-phase single-stage grid tied solar PV ECS using pll-less fast ctf control technique," *IET Power Electronics*, vol. 10, no. 2, pp. 178–188, 2017.
- [5] S. Kumar, A. K. Verma, I. Hussain, B. Singh, and C. Jain, "Better control for a solar energy system: Using improved enhanced phase-locked loop based control under variable solar intensity," *IEEE Industry Applications Magazine*, vol. 23, no. 2, pp. 24–36, March 2017.
- [6] A. M. Rauf and V. Khadkikar, "Integrated photovoltaic and dynamic voltage restorer system configuration," *IEEE Transactions on Sustainable Energy*, vol. 6, no. 2, pp. 400–410, April 2015.
- [7] V. Khadkikar and A. Chandra, "A novel structure for three-phase four wire distribution system utilizing unified power quality conditioner UPQC," *IEEE Trans. Ind. Appl.*, vol. 45, no. 5, pp. 1897–1902, Sept 2009.
- [8] V. Khadkikar, "Enhancing electric power quality using UPQC: A comprehensive overview," *IEEE Trans. Power Electron.*, vol. 27, no. 5, pp. 2284–2297, May 2012.
- [9] B. B. Ambati and V. Khadkikar, "Optimal sizing of upqc considering va loading and maximum utilization of power-electronic converters," *IEEE Trans. Power Del.*, vol. 29, no. 3, pp. 1490–1498, June 2014.
- [10] V. Khadkikar and A. Chandra, "UPQC-S: A novel concept of simultaneous voltage sag/swell and load reactive power compensations utilizing series inverter of UPQC," *IEEE Trans. Power Electron.*, vol. 26, no. 9, pp. 2414–2425, Sept 2011.
- [11] S. Devassy and B. Singh, "Enhancement of power quality using solar pv integrated UPQC," in *39th National Systems Conference (NSC)*, Dec 2015, pp. 1–6.
- [12] S. Devassy and B. Singh, "Modified p-q theory based control of solar PV integrated UPQC-S," in *IEEE Industry Applications Society Annual Meeting*, Oct 2016, pp. 1–8.
- [13] H. Akagi, E. Watanabe, M. Aredes, *Instantaneous Power Theory and Applications to Power Conditioning*. New Jersey: Wiley, 2007.
- [14] P. Kanjiya, B. Singh, A. Chandra, and K. Al-Haddad, "'SRF Theory Revisited' to control self-supported dynamic voltage restorer (dvr) for unbalanced and nonlinear loads," *IEEE Trans. Ind. Appl.*, vol. 49, no. 5, pp. 2330–2340, Sept 2013.
- [15] R. R. Pereira, C. H. da Silva, L. E. B. da Silva, G. Lambert-Torres, and J. O. P. Pinto, "New strategies for application of adaptive filters in active power filters," *IEEE Trans. Ind. Appl.*, vol. 47, no. 3, pp. 1136–1141, May 2011.
- [16] S. Arya and B. Singh, "Performance of DSTATCOM using leaky LMS control algorithm," *IEEE Journal of Emerging and Selected Topics in Power Electronics*, vol. 1, no. 2, pp. 104–113, June 2013.
- [17] B. Singh, S. R. Arya, A. Chandra, and K. Al-Haddad, "Implementation of adaptive filter in distribution static compensator," *IEEE Trans. Ind. Appl.*, vol. 50, no. 5, pp. 3026–3036, Sept 2014.
- [18] R. S. Herrera and P. Salmeron, "Present point of view about the instantaneous reactive power theory," *IET Power Electronics*, vol. 2, no. 5, pp. 484–495, Sept 2009.
- [19] M. Popescu, A. Bitoleanu, and V. Suru, "A dsp-based implementation of the p-q theory in active power filtering under nonideal voltage conditions," *IEEE Transactions on Industrial Informatics*, vol. 9, no. 2, pp. 880–889, May 2013.
- [20] R. Niwas, B. Singh, S. Goel, and C. Jain, "Unity power factor operation and neutral current compensation of diesel generator set feeding three phase four-wire loads," *IET Generation, Transmission Distribution*, vol. 9, no. 13, pp. 1738–1746, 2015.

- [21] P. Rodriguez, R. Teodorescu, I. Candela, A. V. Timbus, M. Liserre, and F. Blaabjerg, "New positive-sequence voltage detector for grid synchronization of power converters under faulty grid conditions," in *Power Electronics Specialists Conference, 2006. PESC '06. 37th IEEE*, June 2006, pp. 1–7.
- [22] S. Golestan, F. D. Freijedo, A. Vidal, A. G. Yepes, J. M. Guerrero, and J. Doval-Gandoy, "An efficient implementation of generalized delayed signal cancellation PLL," *IEEE Trans. Power Electron.*, vol. 31, no. 2, pp. 1085–1094, Feb 2016.
- [23] Y. F. Wang and Y. W. Li, "A grid fundamental and harmonic component detection method for single-phase systems," *IEEE Trans. Power Electron.*, vol. 28, no. 5, pp. 2204–2213, May 2013.
- [24] Y. F. Wang and Y. W. Li, "Three-phase cascaded delayed signal cancellation pll for fast selective harmonic detection," *IEEE Trans. Ind. Electron.*, vol. 60, no. 4, pp. 1452–1463, April 2013.
- [25] M. de Brito, L. Galotto, L. Sampaio, G. de Azevedo e Melo, and C. Canesin, "Evaluation of the main MPPT techniques for photovoltaic applications," *IEEE Trans. Ind. Electron.*, vol. 60, no. 3, pp. 1156–1167, March 2013.
- [26] T.-F. Wu, C.-L. Shen, C.-H. Chang, and J. Chiu, "1  $\phi$ ; 3w grid connection pv power inverter with partial active power filter," *IEEE Transactions on Aerospace and Electronic Systems*, vol. 39, no. 2, pp. 635–646, April 2003.
- T.Satheesh Kumar**, is Post Graduation Scholar in the Department of EEE, Sree Vidyanikethan Engineering college (Autonomous), Tirupathi, Andhra Pradesh, India. He did his Graduation B.Tech from YSR Engineering college of Yogi Vemana University, Proddatur. His areas of interest are Power system Dynamics, Power Electronic convertors and Renewable Energy Sources.
- Kola Leleedhar Rao** is working as Assistant Professor in the Department of EEE, Sree Vidyanikethan Engineering College (Autonomous), Tirupathi, Andhra Pradesh, India. He did Post Graduation, M.Tech, from JNTUA College of Engineering (Autonomous) Anantapur and pursued Bachelor's degree, B.Tech, from S.V. University, Tirupati. He acquired total 11 years of experience in teaching and industry particularly in the area of 400kV EHV Substation & Transmission Line constructions. His areas of research interest include Smart Power Systems & Renewable Energy based Distributed Generation, Power Systems impacts of Future Energy Systems Integration, and Application oriented Electrical systems design and development.

